The insertion loss of screens under the influence of wind

Rasmussen, Karsten Bo; Arranz, Marta Galindo

Published in:
Acoustical Society of America. Journal

Link to article, DOI:
10.1121/1.423853

Publication date:
1998

Document Version
Publisher's PDF, also known as Version of record

The insertion loss of screens under the influence of wind

Karsten B. Rasmussen and Marta Galindo Arranz[a)]
Department of Acoustic Technology, Building 352, Technical University of Denmark, DK-2800 Lyngby, Denmark

(Received 21 September 1997; revised 5 August 1998; accepted 19 August 1998)

Point source propagation over a screen located on a finite impedance surface representative of grass-covered ground is investigated under upwind and downwind conditions. The theoretical part of the investigation involves extended use of parabolic equation methods (PE) allowing for the changes in the vertical wind speed profile when the wind field passes the screen. The influence of turbulence is also implemented. The experimental part of the investigation relies on a scale model technique based upon a 1:25 scaling ratio and a triggered spark source. The main results relate to the size of the insertion loss of a screen under windy conditions and to the acoustic importance of the redirection of the flow before and after the screen. © *1998 Acoustical Society of America.* [S0001-4966(98)06511-4]

PACS numbers: 43.28.Fp, 43.20.Bi [LCS]

INTRODUCTION

The attenuation obtained by means of outdoor sound barriers has been studied in detail for homogeneous and still air.[1–3] The influence of wind and temperature gradients and turbulence has been investigated considerably for the case of sound propagation over plane unobstructed ground,[4–14] but not for screens. In practice the insertion loss will often be influenced by temperature gradients and wind, including turbulence effects, but it appears that only few studies of this exist.[15–19]

In the present work a screen on a finite impedance surface representative of grass-covered ground is investigated experimentally and theoretically under the influence of wind. Upwind as well as downwind conditions are investigated. The experimental data are the result of model experiments in a 1:25 scale model within a boundary layer wind tunnel. The experiments simulate the effect of noise screens located on porous outdoor surfaces for monopole point source propagation. The sound field is measured using a triggered spark source and averaging on a power basis in the frequency domain. The approximate wind field is determined by means of hot-wire anemometry in positions on both sides of the screen, as well as directly over the screen. While the wind tunnel has been improved, the technique of acoustic measurement and flow measurement is as previously described.[19]

The measured data are compared with calculated results obtained by means of parabolic equation methods. Most of the calculations are based upon assumptions of laminar flow while gradual changes of the wind speed profile along the propagation path are taken into account. To some extent the measurements will be influenced by turbulence generated near the ground and additional turbulence generated by the screen. Additional calculations estimating the influence of turbulence when a screen is present are included and the influence of turbulence is discussed and interpreted.

[a)]Present affiliation: CTBTO, IMS, Hydroacoustics, Vienna International Centre, P.O. Box 1250, A-1400 Vienna, Austria.

I. ACOUSTIC PARABOLIC EQUATIONS THEORY

A. Theory for laminar flow

Starting from the Helmholtz equation the family of parabolic differential equations may be derived. For the case of atmospheric propagation this was first done by Gilbert and White.[4] The main stages of the derivation are repeated here for the sake of clarity.

In a constant density medium with symmetry around a vertical axis through the source location we may write the homogeneous Helmholtz equation in cylindrical coordinates,

$$\frac{\partial^2 p}{\partial r^2}+\frac{1}{r}\frac{\partial p}{\partial r}+\frac{\partial^2 p}{\partial z^2}+k_0^2 n^2 p=0, \tag{1}$$

where the refraction index $n(r,z)$ is equal to $c_0/c(r,z)$ and where the pressure is specified as a function of range and height, $p(r,z)$. k_0 is a reference wave number.

Using the $e^{-i\omega t}$ time convention the solution may be written as a product of two functions, one of which is the Hankel function,

$$p(r,z)=H_0^1(k_0 r)\phi(r,z), \tag{2}$$

where ϕ represents the envelope of the outgoing cylindrical wave given by the Hankel function. The envelope is assumed to be slowly varying in range, r.

Under far field conditions this leads to a simplified elliptic equation,

$$\frac{\partial^2 \phi}{\partial r^2}+2ik_0\frac{\partial \phi}{\partial r}+\frac{\partial^2 \phi}{\partial z^2}+k_0^2(n^2-1)\phi=0. \tag{3}$$

The elliptic wave equation may be further transformed. Considering the outgoing part of the field only and exploiting the assumption that the medium is slowly varying with range, the following equation may be obtained:[13]

$$\frac{\partial \phi}{\partial r}=ik_0\left(\sqrt{n^2+\frac{1}{k_0^2}\frac{\partial^2}{\partial z^2}}-1\right)\phi. \tag{4}$$

This equation is an exact one-way equation in the far field for a range independent medium. However, the presence of

the square root, which is a pseudo-differential operator, necessitates further approximation. Different approximate solution methods exist and these are denoted parabolic equation (PE) methods. The approach used in this work is the standard Crank–Nicolson[13,20] wide angle approximation which employs implicit finite difference for marching the solution in range. This approach is slow in comparison with the fast-PE methods[21,22] but it is well suited for treating range dependent effects. The starter used for source representation is a Greene starter.[13,23,24]

The screen was included in the calculations by means of setting the field to zero on the screen surface as originally suggested by Salomons.[17]

B. Theory for turbulent flow

For the sake of the present investigation an approach estimating the influence of turbulence on the acoustic propagation is needed. The approach used in this work was developed by Galindo[13] which in turn follows the ideas from Gilbert *et al.*[8] but with a different implementation.

From Eq. (4), our standard parabolic equation, the refraction index $n(r,z)$ may be rewritten as $n_d+\mu(r,z)$, where n_d is the deterministic component and μ is the stochastic component, and the pseudo-differential operator, Q, may be expressed as

$$Q=\sqrt{1+q}, \quad q=(n_d+\mu)^2+\frac{1}{k_0}\frac{\partial^2}{\partial z^2}-1. \tag{5}$$

q may be written as

$$q=q_d+\mu^2+2\mu n_d, \quad q_d=n_d^2+\frac{1}{k_0}\frac{\partial^2}{\partial z^2}-1, \tag{6}$$

where the right hand equation defines q_d. As a result the parabolic equation may be written as

$$\frac{\partial \phi}{dr}=ik_0(\sqrt{1+q_d+2n_d\mu}-1)\phi, \tag{7}$$

where weak turbulence ($\mu^2 \ll 1$) has been assumed. Expanding the square root for small argument one obtains

$$\sqrt{1+q_d+2n_d\mu}=1+\tfrac{1}{2}(q_d+2n_d\mu)-\tfrac{1}{8}(q_d+2n_d\mu)^2+\cdots. \tag{8}$$

Ignoring small terms one obtains the result

$$\sqrt{1+q_d+2n_d\mu}\approx 1+\tfrac{1}{2}q_d-\tfrac{1}{8}q_d^2+n_d\mu. \tag{9}$$

In this equation the first three terms represent the Taylor expansion of $(1+q_d)^{1/2}$. This means that the pseudo-differential operator, Q, may be written as

$$Q\approx Q_d+n_d\mu, \quad Q_d=\sqrt{1+q_d}. \tag{10}$$

The Crank–Nicolson implicit difference scheme is applied for marching the equation in range. This is a relatively slow approach. This may perhaps be improved by means of the split-step algorithm as proposed in Gilbert *et al.*[8]

In order to introduce the stochastic fluctuations into the calculations it is necessary to introduce the assumption that the two-dimensional autocorrelation function $B_n(s)$ is Gaussian:

$$B_n(s)=\mu_0^2 e^{-|s|^2/L^2}. \tag{11}$$

L is the correlation length (turbulence scale), s is the separation distance in the r-z plane, and μ_0^2 is the variance of μ (turbulence strength).

The wave number spectrum $W(k_r,k_z)$ is defined as the Fourier transform of the autocorrelation function,

$$W(k_r,k_z)=\int\int B_n(s_r,s_z)e^{i(k_r s_r+k_z s_z)}\,ds_r\,ds_z, \tag{12}$$

where k_r and k_z are the radial and the vertical components of the wave number vector, and s_r and s_z are the radial and vertical components of the spatial separation.

From integration of Eq. (12) one obtains the wave number magnitude spectrum,

$$\sqrt{W(k_r,k_z)}=\mu_0 L\sqrt{\pi}e^{-(1/8)(k_r^2+k_z^2)L^2}. \tag{13}$$

$\mu(r,z)$ may be found from inverse Fourier transformation of $(W)^{1/2}$ multiplied by a uniformly distributed random phase function, ψ,

$$\mu(r,z)=\frac{N}{(2\pi)^2}\int\int\sqrt{W(k_r,k_z)}e^{-i(k_r r+k_z z)} \times e^{-i\psi(k_r,k_z)}\,dk_r\,dk_z, \tag{14}$$

where N is a normalization factor given by the square root of the area over which μ is defined. Different randomizations of ψ represent different realizations of the turbulence.[8]

C. Implementation

Fluid mechanics research on flow over obstacles seems to imply that while the velocity profile takes more than 50 screen heights after the screen to recover to the condition before the screen, some sort of logarithmic profile is found again as early as 6 step heights after the screen.[25] Numerical simulations may be carried out based on Navier–Stokes equations taking viscosity into account. No analytical representation of the development of the flow over a vertical screen on a horizontal surface exists[26] except for the approach based on Laplace's equation valid for irrotational flow only.[27] This simplification leads to a flow which is symmetric with respect to the screen. Such a symmetry is by no means present in experimental data as may be inferred from the above statement concerning flow recovery reported by fluid mechanics specialists.

In the present work, the flow is described by logarithmic profiles all the way over the screen. The expression for the sound speed profile is

$$c(z)=c_0+v_0\,\ln\left(\frac{z}{z_0}\right), \tag{15}$$

where c_0 is the sound speed in the absence of wind and $c(z)$ expresses the effective sound speed profile used in simulations. Two different screens are considered, one 2.5 m high, the other 1.25 m high.

An interpolation of the flow parameters v_0 and z_0 determining the sound speed profile is initiated 5 m before the flow arrives at the screen. The vertical profile is gradually modified so that the roughness length, z_0, is equal to the

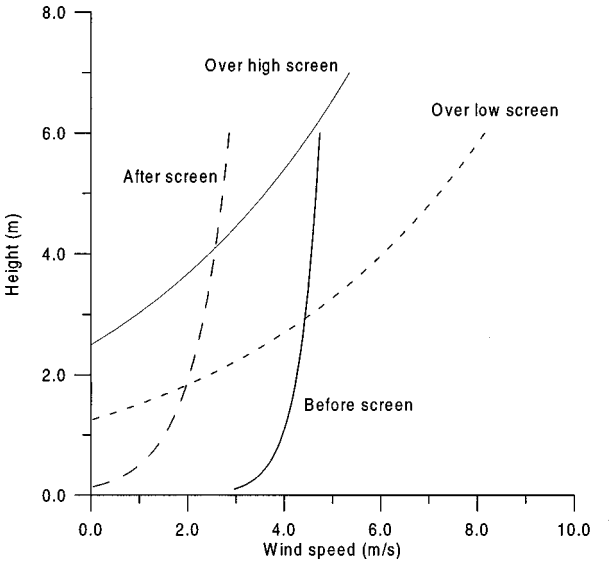

FIG. 1. Analytical approximations for wind speed profiles.

screen height at the screen position. The transition is based on simple linear interpolation of the values of (v_0, z_0). The interpolation is determined by $(v_0, z_0) = (0.4341, 0.000\,108\,3)$ at 5 m before screen, $(v_0, z_0) = (5.2, 2.5)$ at high screen or $(v_0, z_0) = (5.2, 1.25)$ at low screen. The values for the parameters (v_0, z_0) are determined from flow measurements and $(0.4341, 0.000\,108\,3)$ represents flow for unobstructed terrain, whereas the values given at the screen position represent the flow at this position for the two screen heights.

After the flow has passed the screen, a similar transition is used but the interpolation is carried out in a zone extending to 15 m after the screen. Hence, the rate of change of the profile is taken to be three times slower after the screen than before the screen. At 15 m $(v_0, z_0) = (0.7498, 0.1321)$. These parameter values lead to the curves in Fig. 1.

It should be stressed that the transition of flow close to the screen is only modeled in a very simplified way by these considerations but a more accurate description is not easily found.

The ground was characterized by flow resistivity and layer thickness (full scale values) in the impedance model described by Attenborough[28] as the 2PA model. In the present notation $(e^{-i\omega t})$ it reads thus:

$$Z(\sigma,\beta) = \sqrt{\frac{\sigma}{f}}\,0.4342(1+i) + i\,\frac{\beta}{f}\,9.6485, \tag{16}$$

where convenient values have been inserted for sound speed (340 m/s), density (1.204 13 kg/m^3), and ratio of specific heats (1.4021). The parameter Z denotes the relative characteristic impedance and β denotes the rate of exponential decrease of porosity with depth. Alternatively β may be interpreted as $2/d_e$, where d_e is the effective thickness of a porous layer of constant porosity on a hard backing. σ is the flow resistivity.

The PE calculations are based upon the use of 8 points per wavelength horizontally as well as vertically and a total of 4000 vertical discretization points.

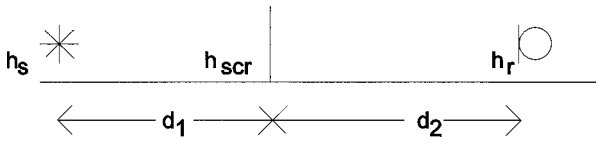

FIG. 2. Full scale geometrical parameters. $h_s = 1.5$ m in all cases.

II. RESULTS

A. Meteorological data from scale model

The meteorological data are obtained from Dantec Streamline hot-wire anemometry equipment (using a type 55p11 single wire probe). The wind speed is found as an average over 54 s. A meteorological sampling rate of 300 Hz was used; this rate was found to be more than sufficient. The anemometer probes were positioned with a vertical wire to obtain measured data that was insensitive to vertical flow.

The wind speed profile was measured in positions (converted to full scale) 12.5 m before the flow reaches the screen; another profile measurement was made just above the screen and in positions 12.5 m after the screen. The logarithmic wind speed profiles obtained by curve fitting are shown in Fig. 1. Note that the speed above the screen is higher than before and after the screen as a consequence of the redirection of the flow caused by the screen.

B. Comparison with acoustical data from scale model

The acoustic measurements are based on energy averaging in the frequency domain of 12 pulses, each of which has been edited in the time domain so that reflections from tunnel walls, etc. are removed. Energy averaging is necessary because of the stochastic process involved in propagation under the influence of wind. The frequency range of the measured data is limited to between 125- and 3000-Hz full scale—the frequency range where the signal-to-noise ratio was satisfactory. The basic setup involving the screen is shown in Fig. 2. The thickness of the model screen was 9 mm corresponding to 22.5 cm in full scale. Equation (16) was used to describe the acoustic impedance of the ground surface (which was a layer of very open synthetic material on top of a thin cotton material on hard backing) with $\sigma = 7$ kNsm^{-4} and $\beta = 125$ m^{-1} for full scale frequencies. The value of β corresponds to a homogeneous porous layer of thickness $d_e = 2/\beta = 0.0160$ m on a hard backing. This full scale thickness is approximately 25 times the physical thickness of the material used in the scale model. The choice of parameter values in the 2PA model is the result of curve-fitting sound pressure level results as a function of full scale frequency for the case without wind and for unobstructed terrain.

The measured results shown in the figures are all scale model data which are shown in a full scale context. Hence, all frequencies and heights and distances refer to full scale conditions. The source height is 1.5 m in all cases. Figure 3 shows relative sound pressure levels for an unscreened case with a wind speed profile as shown in Fig. 1 (curve labeled ''before screen''). The agreement between measured data and calculated values is seen to be quite good except for

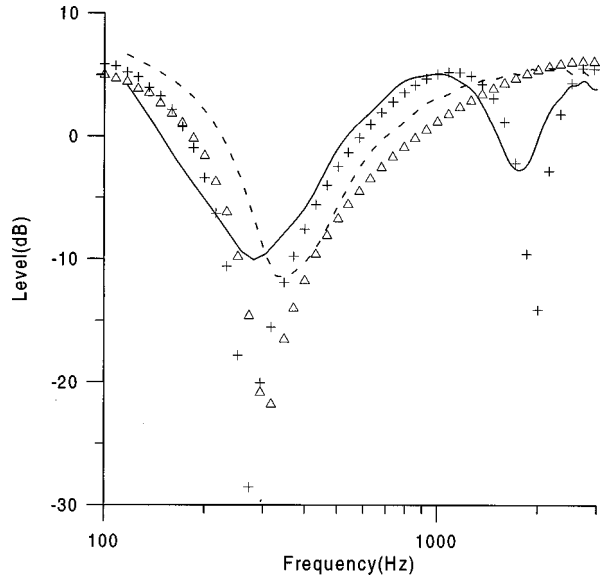

FIG. 3. Sound pressure level relative to free field. $h_{scr}=0$, $h_r=2.5$ m, $d_1+d_2=60$ m. Full line, measured for downwind; +, calculated for downwind; dashed line, measured for upwind; △, calculated for upwind.

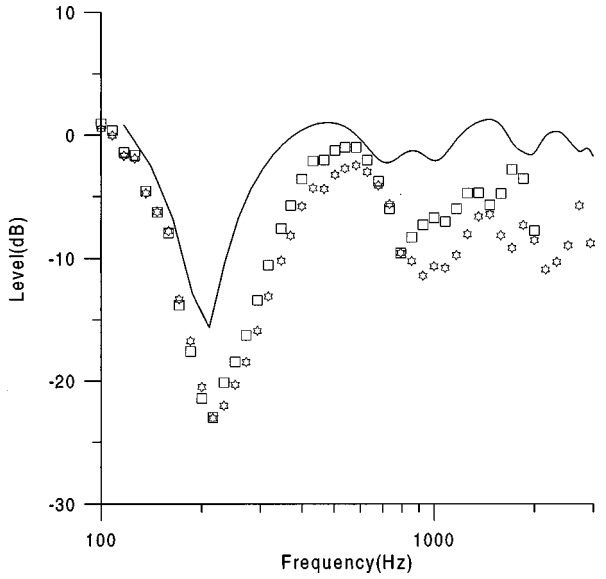

FIG. 5. Sound pressure level relative to free field. $h_{scr}=2.5$, $h_r=2.5$ m, $d_1=25$ m, $d_2=35$ m. Full line, measured for downwind; calculated for downwind (□) based on 5-m flow transition zone upstream of screen and 15-m transition zone downstream of screen. Additional calculations (☆) for discontinuous wind speed profile (no transition zone).

frequencies where the level has a sharp minimum. (Results without wind and measured over a similar acoustic surface may be found in previous work[3] and they also agree well with calculated data from the 2PA model.)

In Fig. 4 the distance from source to screen is 25 m and from screen to receiver 35 m. The screen height is 1.25 m and the receiver height is 0.5 m. The calculations are for laminar wind flow. The agreement between measured and calculated data is good, especially for no wind.

In Figs. 5 and 6 the distances and heights are the same as in Fig. 4 except for the screen height which is now increased to 2.5 m and the receiver height which is increased to 2.5 m. It should be noted that Figs. 5 and 6 show results of two slightly different calculations. Either a transition zone of 5 m before and 15 m after the flow passes the screen is included in the simulations taking the wind into account, or the wind profile is considered to change abruptly at the screen location. The former approach is a simulation of the actual flow conditions near the screen, whereas the latter approach treats the wind speed profiles as constant from source to screen and again from screen to receiver. The results indicate that the simple discontinuous approach is insufficient for higher frequencies, and also that better agreement is obtained for upwind than for downwind. This is a general trend and is re-

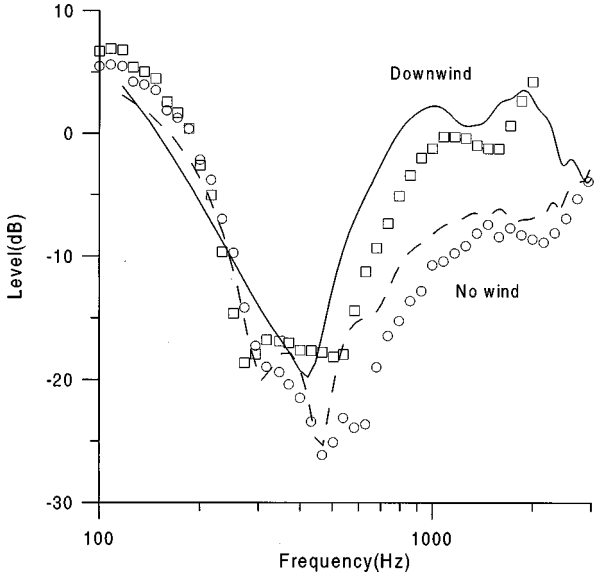

FIG. 4. Sound pressure level relative to free field. $h_{scr}=1.25$, $h_r=0.5$ m, $d_1=25$ m, $d_2=35$ m. Full line, measured for downwind; □, calculated for downwind; dashed line, measured for nowind; ○, calculated for nowind. Calculations for wind based on 5-m flow transition zone upstream of screen and 15-m transition zone downstream of screen.

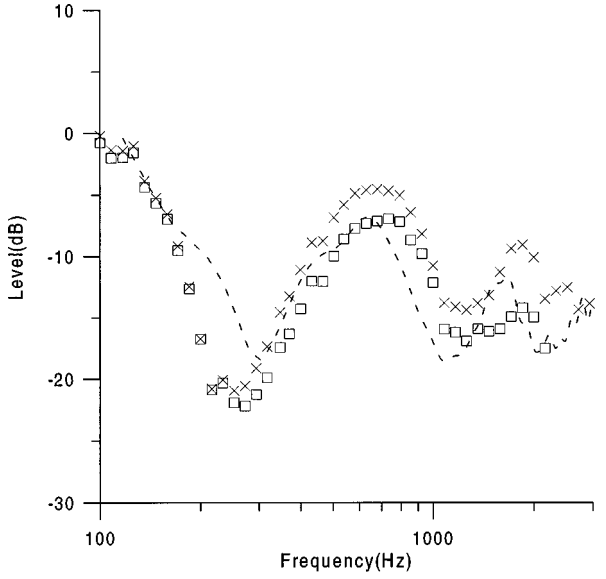

FIG. 6. Sound pressure level relative to free field. $h_{scr}=2.5$, $h_r=2.5$ m, $d_1=25$ m, $d_2=35$ m. Interrupted line, measured for upwind; calculated for upwind (□) based on 5-m flow transition zone upstream of screen and 15-m transition zone downstream of screen. Additional calculations (×) for discontinuous wind speed profile (no transition zone).

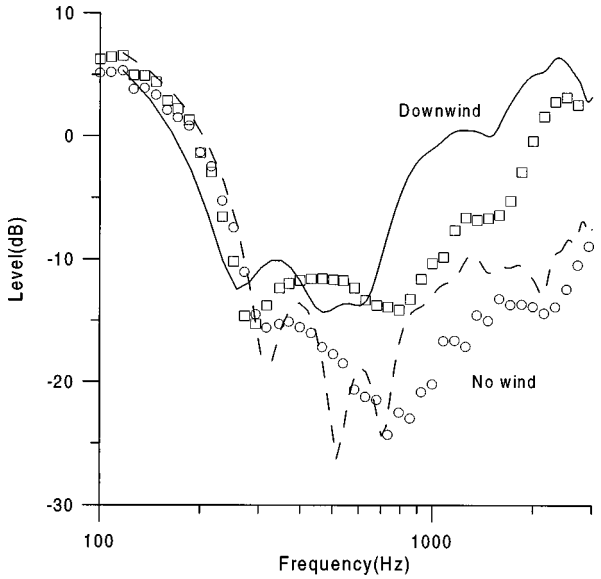

FIG. 7. Sound pressure level relative to free field. $h_{scr}=1.25$, $h_r=0.25$ m, $d_1=25$ m, $d_2=25$ m. Full line, measured for downwind; □, calculated for downwind. Calculations for wind based on 5-m flow transition zone upstream of screen and 15-m transition zone downstream of screen. Interrupted curve, measured for no wind; ○, calculated for no wind.

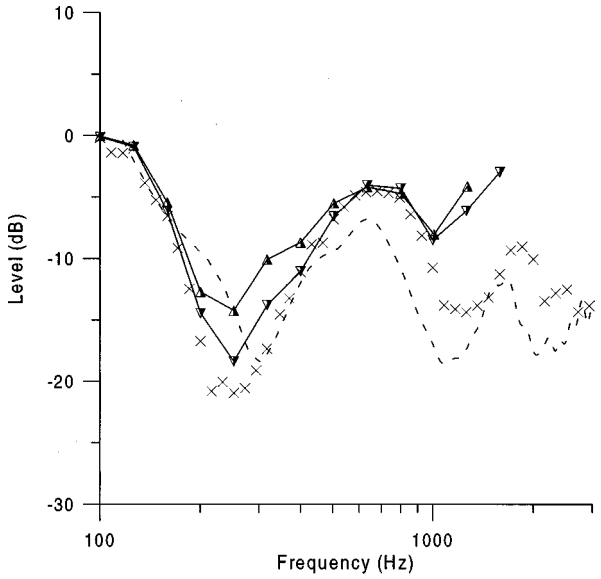

FIG. 8. Sound pressure level relative to free field. $h_{scr}=2.5$, $h_r=2.5$ m, $d_1=25$ m, $d_2=35$ m. Interrupted line, measured for upwind; ×, calculations for discontinuous wind speed profile (no transition zone). Triangles denote calculations including turbulence effect for ten realizations. Turbulence is assumed to originate from the screen and is taken into account until 10 m after the flow has passed the screen. $\mu_0^2=0.0002$. Triangles base down: correlation length $L=1.1$; base up: $L=0.4$.

lated to the asymmetry of the flow pattern close to the screen. When the extended transition region is on the receiver side (i.e., for downwind) the acoustic results become sensitive to the lack of a precise flow representation in the region.

An additional example is shown in Fig. 7 representing the case where the distance from screen to receiver is reduced to 25 m. The low screen height of 1.25 m is used and the receiver height is only 0.25 m. The distance from source to screen is still 25 m.

Experimental evidence obtained using the anemometer equipment and correlation analysis as suggested by Daigle *et al.*[6] shows that the full scale correlation length, L, is approximately 0.4 m, and that μ_0^2 is of the order 3×10^{-6} measured as the variance of the wind speed divided by the sound speed squared. Strictly speaking, the scale modeling technique is not applicable when turbulence is considered, since turbulence effects do not scale. The primary reason for this is that the viscous properties of the fluid are not scaled.[27] It must be added, however, that the correlation length usually found in outdoor experiments without screens is around 1.1 m, and μ_0^2 is usually close to 2×10^{-6}, values that are close to those obtained from the scale model experiment. Numerical simulations according to the method described in Sec. I B have shown negligible influence from turbulence using the abovementioned values. The turbulence calculation example included as Fig. 8 is made for exaggerated turbulence values in order to show the qualitative influence. It is seen that the interference minima are affected as could be expected.

The measured and calculated insertion loss of the screens are displayed directly in Figs. 9 and 10 valid for downwind and upwind, respectively, for a 2.5-m screen. The agreement between measured and calculated results is quite good, especially for upwind. For downwind the results show that the insertion loss fluctuates around zero. This is in agreement with findings of Scholes *et al.*[16] who measured the influence of screens (full scale measurements) and who found that in a downwind situation the insertion loss was not always positive.

III. CONCLUSIONS

The primary conclusion of the present work is that the experiments infer that the applied PE method is applicable to the combined effect of screens and wind provided that sufficient information about the wind field is present. This result is not trivial since a number of approximations are inherent

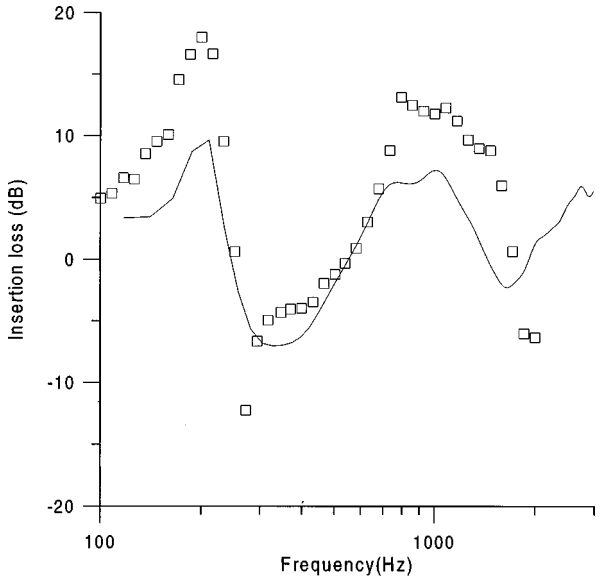

FIG. 9. Insertion loss for downwind based upon data from Figs. 3 and 5. Full line, measured; □, calculations for wind based on 5-m flow transition zone upstream of screen and 15-m transition zone downstream of screen.

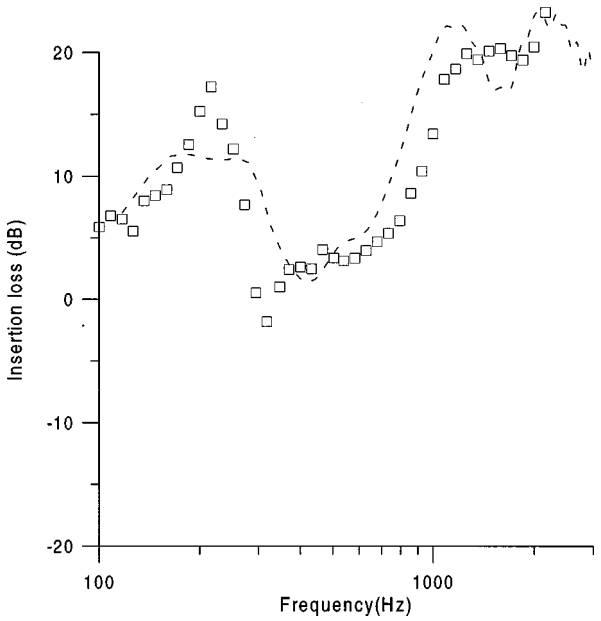

FIG. 10. Insertion loss for upwind based upon data from Figs. 3 and 6. Interrupted line, measured; □, calculations for wind based on 5-m flow transition zone upstream of screen and 15-m transition zone downstream of screen.

in the numerical approach used, namely one-way propagation only, decreasing accuracy as the acoustic emission angle reaches around 40 degrees measured from horizontal (this is a combination of the PE approach and the choice of starter representing the source field). These are the fundamental PE limitations. In addition to that the screen is included in the calculations in a nonrigorous manner and the mere presence of the screen is in conflict with the assumption included in the PE approach that the topography must only change slowly.

Additional problems are related to the wind field. It is very difficult to make an accurate implementation of a wind speed profile which develops with distance in a realistic manner. And lastly the turbulence is taken into account in (some of) the calculations but based on assumptions of Gaussian distributions and of weak turbulence only.

The most important problem is believed to be the problems related to the wind field. Results in other publications[1–3] have shown that when no wind is present, very satisfactory results for the sound pressure level behind screens may be obtained. Trying to understand the details of that limitation, it may be said that the complicated flow pattern (laminar flow) was more important to the results than hitherto supposed, and for the results presented here the turbulence seems to play a less significant role than previously believed.[18]

The experiments presented in this work are meant to be representative of full scale noise barriers. Such a transformation of results is likely to cause inaccuracies, and for the case of turbulence it is in fact known to be inaccurate since the viscous properties of the fluid are not scaled. It is unlikely, however, that the deviations related to the incomplete scaling will affect the overall tendencies in the results obtained for flow. On the basis of the results obtained in this work it therefore is reasonable to expect the exact flow pattern close to a noise screen to be important for the insertion loss. This means that the flow pattern associated with a specific noise screen design could be an important parameter. Previous studies of the influence of the screen shape in a still and homogeneous atmosphere[1] should in the future be supplemented by studies taking the wind flow over the screen into account.

[1] D. C. Hothersall, S. N. Chandler-Wilde, and M. N. Hajmirzae, ''Efficiency of single noise barriers,'' J. Sound Vib. **146**, 303–322 (1991).
[2] D. J. Saunders and R. D. Ford, ''A study of the reduction of explosive impulses by finite sized barriers,'' J. Acoust. Soc. Am. **94**, 2859–2875 (1993).
[3] K. B. Rasmussen, ''Model experiments related to outdoor sound propagation over an earth berm,'' J. Acoust. Soc. Am. **96**, 3617–3620 (1994).
[4] K. E. Gilbert and M. J. White, ''Application of the parabolic equation to sound propagation in a refracting atmosphere,'' J. Acoust. Soc. Am. **85**, 630–637 (1989).
[5] K. B. Rasmussen, ''Computer simulation of sound propagation over ground under the influence of atmospheric effects. Letter to the editor,'' J. Sound Vib. **141**, 347–354 (1990).
[6] G. A. Daigle, J. E. Piercy, and T. F. W. Embleton, ''Effects of atmospheric turbulence on the interference of sound waves near a hard boundary,'' J. Acoust. Soc. Am. **64**, 622–630 (1978).
[7] G. A. Daigle, ''Effects of atmospheric turbulence on the interference of sound waves above a finite impedance boundary,'' J. Acoust. Soc. Am. **65**, 45–49 (1979).
[8] K. E. Gilbert, R. Raspet, and X. Di, ''Calculation of turbulence effects in an upward-refracting atmosphere,'' J. Acoust. Soc. Am. **87**, 2428–2437 (1990).
[9] M. R. Stinson, D. I. Havelock, and G. A. Daigle, ''Comparison of predicted and measured sound pressure levels within a refractive shadow in the presence of turbulence,'' Proceedings of Inter-Noise 95, July 10–12, 1995 (Newport Beach, CA, 1995), pp. 327–330.
[10] A. L'Espérance, Y. Gabillet, and G. A. Daigle, ''Outdoor sound propagation in the presence of atmospheric turbulence: Experiments and theoretical analysis with the fast field program algorithm,'' J. Acoust. Soc. Am. **98**, 570–579 (1995).
[11] R. Raspet and Wenliang Wu, ''Calculation of average turbulence effects on sound propagation based on the fast field program formulation,'' J. Acoust. Soc. Am. **97**, 147–153 (1995).
[12] P. Chevret, Ph. Blanc-Benon, and D. Juvé, ''A numerical model for sound propagation through a turbulent atmosphere near the ground,'' J. Acoust. Soc. Am. **100**, 3587–3599 (1996).
[13] Galindo Arranz, ''The parabolic equation method for outdoor sound propagation,'' Department of Acoustic Technology, DTU, Report No. 68 (1996).
[14] V. E. Ostashev, G. Goedeke, F. Gerdes, R. Wandelt, and J. Noble, ''Line-of-sight sound propagation in the turbulent atmosphere with Gaussian correlation functions of temperature and wind velocity fluctuations,'' *Proceedings of Seventh Int. Symp. on Long Range Sound propagation*, Ecole Centrale de Lyon, 24–26 July 1996, Lyon, France, pp. 339–357.
[15] R. DeJong and E. Stusnick, ''Scale model studies of the effects of wind on acoustic barrier performance,'' J. Noise Control Eng. **6**, 101–109 (1976).
[16] W. E. Scholes, A. C. Salvidge, and J. W. Sargent, ''Field performance of a noise barrier,'' J. Sound Vib. **16**, 627–642 (1971).
[17] E. M. Salomons, ''Diffraction by a screen in downwind sound propagation: A parabolic-equation approach,'' J. Acoust. Soc. Am. **95**, 3109–3117 (1994).
[18] K. B. Rasmussen and M. Galindo Arranz, ''Scale model investigations into the insertion loss of screens under the influence of wind,'' J. Acoust. Soc. Am. **100**, 2589(A) (1996).
[19] K. B. Rasmussen, ''Sound propagation over screened ground under upwind conditions,'' J. Acoust. Soc. Am. **100**, 3581–3586 (1996).
[20] D. Lee and S. T. McDaniel, *Ocean Acoustic Propagation by Finite Difference Methods* (Pergamon, New York, 1988).
[21] K. E. Gilbert and Xiao Di, ''A fast Green's function method for one-way sound propagation in the atmosphere,'' J. Acoust. Soc. Am. **94**, 2343–2352 (1993).
[22] M. Galindo, M. R. Stinson, and G. Daigle, ''Comparison of some methods

used for prediction of atmospheric sound propagation,'' Canadian Acoustics **25**, 3–12 (1997).
[23] R. R. Greene, ''The rational approximation to the acoustic wave equation with bottom interaction,'' J. Acoust. Soc. Am. **76**, 1764–1773 (1984).
[24] F. B. Jensen, W. A. Kuperman, M. B. Porter, and H. Schmidt, *Computational Ocean Acoustics* (AIP Press, New York, 1994).
[25] H. Le, P. Moin, and J. Kim, ''Direct numerical simulation of turbulent flow over a backward-facing step,'' J. Fluid Mech. **330**, 349–374 (1997).
[26] N. O. Jensen, Risø National Laboratory, Risø, Denmark, Personal communication (1997).
[27] B. S. Massey, *Mechanics of Fluids* (Van Nostrand Reinhold, U.K., 1983), 5th ed.
[28] Equation (12) in K. Attenborough, ''Ground parameter information for propagation modeling,'' J. Acoust. Soc. Am. **92**, 418–427 (1992).